VOL. 11, NO. 2, JANUARY 2016 ISSN 1819-6608
ARPN Journal of Engineering and Applied Sciences

www.arpnjournals.com

INVESTIGATIONS OF THE MIXED MODE CRACK GROWTH BEHAVIOR OF AN ALUMINUM ALLOY

Husaini[1], Kikuo Kishimoto[2], Munetsugu Hanji[3] and Mitsuo Notomi[4]
[1]Department of Mechanical Engineering, Syiah Kuala University, Darussalam, Banda Aceh, Indonesia
[2]Department of Mechanical and Control Engineering, Tokyo Institute of Technology, Meguro-ku, Tokyo, Japan
[3]Honda Motor Co., Ltd., 2-1-1 Aoyama, Minato-ku, Tokyo, Japan
[4]Department of Mechanical Engineering, Meiji University, Kawasaki, Kanagawa, Japan
E-Mail: husainiftm@unsyiah.ac.id

ABSTRACT

Fracture behavior of aluminum alloys under mixed mode (Mode I+II) loading was studied. Fracture tests were carried out on A2024-T351 aluminum. Compact-tension-shear specimen was employed and angle between loading axis and the crack surface was varied from 90° (mode I) to 0° (mode II). The crack extension (crack initiation and propagation) behaviors observed by a video microscope. Under a load with relatively high mode II components, the shear type crack initiation preceded the opening type crack propagation. Final fracture was occurred by shearing instability in the pure mode II loading. The critical values of stress intensity factors at crack initiation under mode II dominant conditions become smaller than those predicted by the maximum hoop stress criterion. Shear type fracture instability occurs at the ligament when the shear stress is over the shear strength of the material. It was also found that the rolling direction and a small holes existing ahead of the crack-tip influence the crack extension behaviors.

Keywords: crack growth behavior, aluminum alloy, shear type fracture, critical stress intensity factor.

INTRODUCTION

In the theoretical analyses of the mixed mode fracture problem the basic assumption was that the stress field near the crack tip is solely determined by the linear elastic fracture mechanics (LEFM). Among others the hypotheses involved the maximum hoop stress criterion stating that fracture occurs when a critical circumferential stress, referred to a polar coordinate system, is reached at some fixed distance from the crack tip. When dealing with materials exhibiting fibrous fracture the question of how to make a reasonable judgment of the crack growth conditions becomes more precarious [1, 2].

Shear fracture in aluminum alloy and polymer alloy under various mixed mode loading conditions were recently reported by Aoki *et al*., [3] and by Husaini *et al*. [4-6], respectively. Aoki *et al*. conducted an elastic-plastic fracture behavior of an aluminum alloy A5083-O under mixed mode loading and pointed out that under mixed mode loading with high mode II components, crack due to shear type fracture initiate at the sharpened corner of the pre-crack tip near the surfaces of a specimen. Husaini *et al*. [4-6], studied the fracture behavior of both ABS and PC/ABS blends under mixed mode loading and suggested that crack initiation occurs in the opening type fracture for the fracture test from mode I to mixed mode loading up to a certain value of mode II component. However, at a certain value of mixed mode ratio with high in mode II components, crack due to shear type fracture initiate at the initial crack tip.

In the present paper, an experimental investigation is made to clarify crack extension behavior of A2024-T351 aluminum alloy. The compact-tension-shear (CTS) specimens are employed to perform the Mode I and Mixed Mode testing. Angle between loading axis and the initial crack was varied from 90° (mode I) to 0°(mode II). Crack growth behaviors near the crack tip were observed by using a video microscope.

In this study, effects of small holes with one hole ahead of the crack tip were also studied. The experimental results were explained by taking into account of the shear type of fracture and maximum hoop stress criterion near the crack tip.

EXPERIMENTS

An aluminum alloy A2024-T351 was tested. Tensile testing was performed in the longitudinal (TL) or rolling direction (RD) and transverse (LT) orientations to obtain stress-strain relationship. It should be noted that the final failure was a shear rupture with the fracture surface incline 45º to the loading direction both of RD (TL) and LT orientations. The mechanical properties of the material are shown in Table-1.

Table-1. Mechanical properties.

Specimen orientation	TL	LT
Young's modulus E [GPa]	73.4	74.4
Poisson's ratio ν	0.34	0.33
Ultimate tensile strength σ_B [MPa]	471	476
0.2 % Yield strength $\sigma_{0.2}$ [MPa]	358	328
Rupture strength σ_f [MPa]	450	473
Shear strength τ_f [MPa]	183	193
Failure strain ε_B [%]	0.17	0.21
Reduction of area δ [%]	19.5	20.3

In the fracture testing CTS specimens were used. Based on the JSME Standard Method of Test for Elastic-Plastic Fracture Toughness J_{IC}-S001 1981[7], a fatigue crack was introduce up to $a_o/w \cong 0.5$ (a_o = pre-cracked length, w = specimen width) from a machined chevron notch as shown in Figure-1.

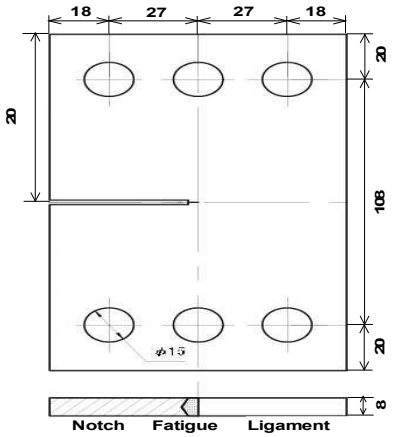

Figure-1. Configuration of a CTS specimen.

After a special loading device developed by Richard and Benitz [8] was attached, as shown in Figure-2, the specimen was loaded in displacement-controlled by MTS testing machine at a constant crosshead rate of 0.3 mm/min.

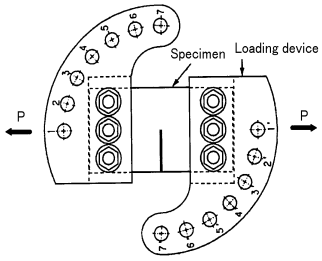

Figure-2. A device for mixed mode loading.

A pure mode I loading was performed using the No. 1 and 1' holes in the loading device (Figure-2), and a pure Mode II loading was carried out using the No. 7 and 7' holes. Angle between loading axis and the initial crack was varied from $\alpha = 90°$(mode I) to $\alpha = 0°$(mode II). Fracture tests were tested in two types of CTS specimens those are in the longitudinal (TL) and transverse (LT) orientations. Moreover, effects of a small hole ahead of the crack tip on the specimens were also tested. The diameter of small holes 6 mm and distance from crack tip to the hole is about 11 mm.

Crack initiation and crack growth at the crack tip were monitored by means of a video microscope. To prevent light reflection from the specimen during observation in the fracture test then it was white painted on both sides of the observation surface.

In order to find stress intensity factor, a numerical analyses of CTS specimen were conducted using a two-dimensional finite element analysis with eight-nodded isoparametric elements. In the FEM model, meshes adjacent to the crack tip of a specimen were divided into fine mesh geometris. These elements were degenerating down to triangles to represent the square root stress singularity. The node at the crack tip was normally tied and the mide-side nodes were moved to the ¼ point [9]. Both calculation and finite element mesh generation are conducted by employing the MARC-MENTAT program [10].

RESULTS AND DISCUSSIONS

Crack Growth Behavior

Figure-3 shows the sequence of pictures taken from video recording of crack growth on the specimen with LT orientation under mode I with $\alpha = 90^o$.

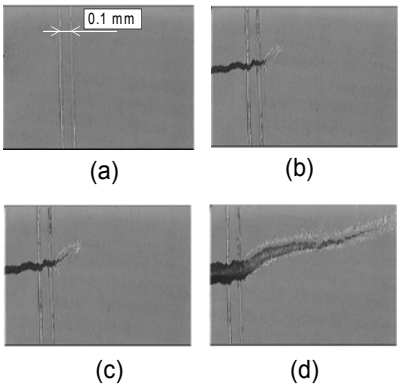

Figure-3. Pictures taken from video recording of crack extension for LT specimen with $\alpha = 90^o$ (Mode I).

It can be seen the scale of about 0.1 mm from the initial crack tip at the surface of the specimen as shown in Figure-3 (a). This scale is used to identified crack initiation easily. Initial state before crack initiation is shown in frame (a). Then, it is just onset the crack initiation at the surface as shown in frame (b). Frame (c) just shows after crack initiation. Crack propagation shows in frame (d). Crack initiation direction as shown in frame (b) look like different angle with the initial crack tip on the surface due to shear lip deformation. On the contrary, in the middle of thickness crack propagates parallel to the initial crack and flat fracture. From these results, it could be suggested that the main mechanism of crack extension is occurred in the opening type fracture. Since a crack initiation occurred at the mid thickness, then it cannot be observed directly. Therefore, instead of that we identified the crack initiation on the surface by video recording as shown in frame (b). On the TL specimen, crack propagates parallel to the initial crack, which is also in flat fracture due to the rolling direction or grain orientation.

Figure-4 shows the pictures taken from video recording of sequence of deformation and fracture process in the vicinity of the crack tip on the specimen with LT orientation under mixed mode with $\alpha = 45^o$.

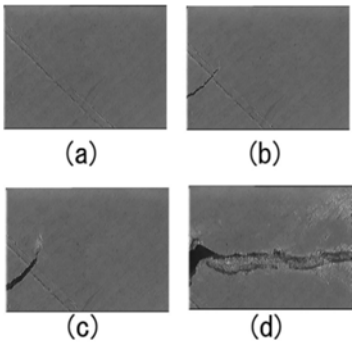

Figure-4. Pictures taken from video recording of crack extension for LT specimen with $\alpha = 45^o$ (Mixed mode).

From the figure, it can be seen that frame (a) shows the initial condition before crack initiation. Frame (b) shows onset the crack initiation occurring in shear type fracture. After initiation, then crack propagates with kink in the 45^o direction (shear type fracture) firstly and then decrease to mode I (opening type fracture) as shown in frame (c). Finally, crack growth occurs in opening type fracture until final failure with the direction perpendicular to the loading axis as shown in frame (d). However, crack extension behavior under mixed mode loading with mode II component higher than mode I, for loading angle $\alpha = 30^o$ and $\alpha = 15^o$, almost similar to fracture behavior with $\alpha = 45^o$ (Figure-4).

Figure-5 shows the sequence of deformation and fracture process around the crack tip taken from video recording on the specimen with LT orientation under pure mode II with loading angle $\alpha = 0^o$.

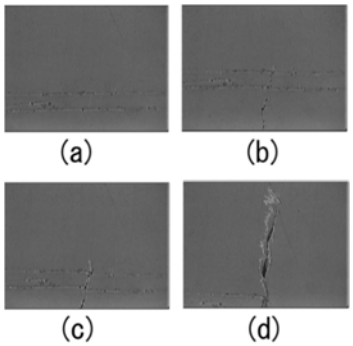

Figure-5. Pictures taken from video recording of crack extension for LT specimen with $\alpha = 0^o$ (pure Mode II).

It can be seen from the Figure-5, frame (a) shows the initial condition before crack initiation. Frame (b) just onset the crack initiation occurring in shear type fractture. Crack propagation was also occurred in shear type fracture as shown in frame (c). Finally, crack growth occurs in shear type fracture until final failure as shown in frame (d). Crack propagates parallel to initial crack and fracture surface is flat and it is similar to the tensile test. These results suggested that it was found a quite diffenrent phenomenon with previous results of A5083-O aluminum alloy [3] and PC/ABS polymer alloy [4] which comes from microstructure.

Crack propagation angle ϕ was measured at 5 mm from the crack tip in the same direction with crack extension. The results of crack propagation direction for complete range from pure mode I ($\alpha = 90^o$) to pure mode II ($\alpha = 0^o$) are plotted in Figure-6.

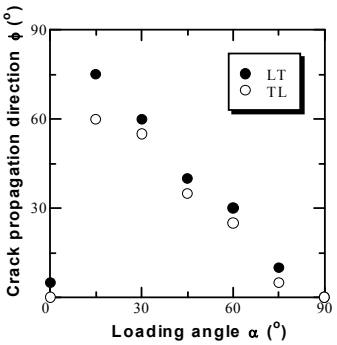

Figure-6. Loading angle α vs. crack direction ϕ.

The data are plotted in the figure both LT and TL specimens. It can be seen in Figure-6, crack propagation direction under mode I and mixed mode with lower in mode II component propagates perpendicular to the loading direction in opening type fracture. Furthermore, crack propagation direction, under mixed mode with higher in mode II component with loading angle α=15°, is perpendicular to loading direction for LT specimen.

Nevertheless, the angle of crack propagation direction ϕ for TL specimen is a slightly small compared to LT specimens. It was found that crack direction parallel both to the loading direction and initial crack tip of LT and TL specimen under pure mode II loading and specimens fracture only in shear type fracture.

Comparison of crack propagation direction between LT and TL specimen under mixed mode with loading angle α=15° are shown in Figure-7.

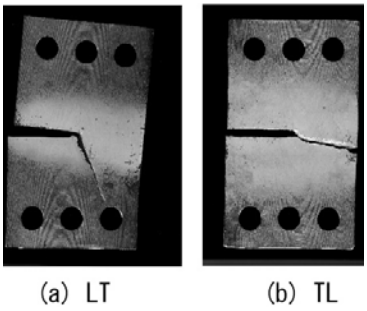

Figure-7. Comparison of crack propagation direction between LT and TL specimen (loading angle α=15°).

It can be seen from the figure that crack propagation direction is perpendicular to the loading direction for LT specimen and fracture occurred in opening type as shown in Figure-7(a). However, crack propagation direction for TL specimen is different from LT specimen since in the TL specimen transition fracture occurred from opening to shear type fracture and final failure caused by shear fracture as shown in Figure-7(b).

Fracture Toughness

Figure-8 shows load-displacement relationship curve under mode I, mixed mode (α=75°) and mode II loading. A small open symbol (O) on the curve indicates the load corresponding to the crack initiation identified previously by video recording as shown in frame (b) of Figure 3, 4, and 5. It shows that crack initiation occurs below maximum load. In addition, crack initiation occurs on the linear parts of load-displacement relationship. Therefore, the small scale yielding fracture criterion could be applied.

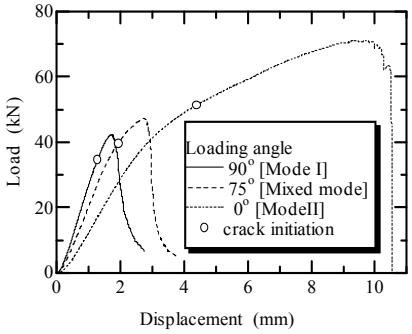

Figure-8. Load versus load-point-displacement curve of LT specimen.

The critical stress intensity factors K_I at crack initiation under mode I loading [11] denoted as K_{Iin}. Hereafter, critical stress intensity factors, which are obtained by this method, will be referred to as fracture toughness K_{Iin} as well as reported in the previous work [12]. It was found that fracture toughness K_{Iin} = 51.5 MPa.m$^{1/2}$ and 45.2 MPa.m$^{1/2}$ of LT and TL specimen, respectively.

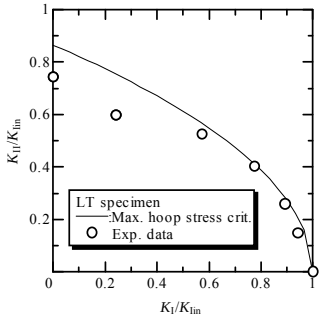

Figure-9. Critical stress intensity factor of LT specimen.

Critical stress intensity factors at crack initiation are shown in Figure-9 for LT specimen where both axes are normalized by fracture toughness K_{Iin}. A critical stress intensity factor at crack initiation for TL specimen is

shown in Figure-10. A solid line in the figures indicates the fracture boundary curve corresponding to the maximum hoop stress criterion $\sigma_{\theta \max.}$ [1].

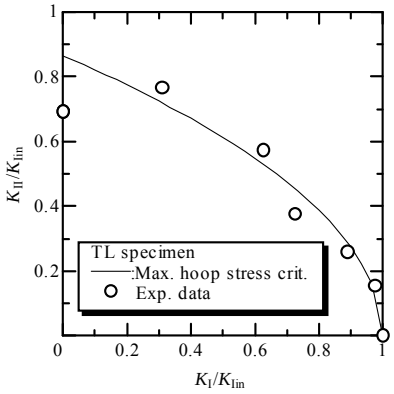

Figure-10. Critical stress intensity factor of TL specimen.

In this criterion, relationship between K_I and K_{II} given by

$$\left(\frac{K_I}{K_{Ic}}\cos^2\theta_0 - \frac{3}{2}\frac{K_{II}}{K_{Ic}}\sin^2\theta_0\right)\cos\frac{\theta_0}{2} = 1, \quad (1)$$

where θ_0 denotes the direction at which hoop stress takes its maximum value, and given by

$$\theta_0 = \sin^{-1}\left(\frac{\kappa}{\sqrt{1+9\kappa^2}}\right) - \tan^{-1} 3\kappa \quad (2)$$

with the mixed mode ratio, $\kappa = K_{II} / K_I$.

Figure-9 and 10 show that the experimental data follow the maximum hoop stress criterion only under pure mode I and mixed mode loading at a certain value of mode II component. This fracture process is also suggested by experimental data as shown in Figure-7(a). On the other hand, when the mode II component exceeds some critical value, it was found that the fracture resistance of tested material decreases in LT specimen as shown in Figure-9.

However, in the TL specimen the fracture resistance decreases at higher in mode II component as shown in Figure-10. This fracture behavior is related to fracture process due to the appearance of opening fracture then followed by shear fracture. From the experimental point of view, these phenomena are also shown in Figure-7(b). In order to predict the direction of crack extension under mixed mode with higher in mode II component of both LT and TL specimen (Figure-7), hence the results were explained experimentally by taking into account of the shear fracture and maximum hoop stress criterion near the crack tip. It can be inferred that, crack extension can be estimated that crack is going to propagate in the direction where strength of material locally is weak. In this case, the weakest of fracture resistance is in the direction parallel or almost parallel to the rolling direction.

Effects of a Small Hole

Figure-11 shows crack propagation behavior for LT specimen with a hole ahead of crack tip under pure mode I, mixed mode, and pure mode II loading as shown in frame (a), (b) and (c), respectively. Arrow in the figure indicates loading direction. The hole with diameter of about 6 mm is introduced 11 mm ahead of initial crack tip.

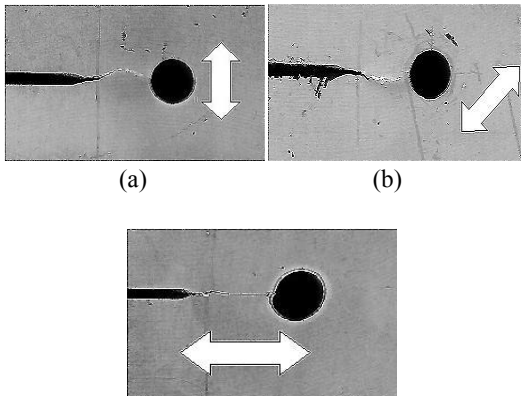

Figure-11. Crack propagation behavior of LT specimen with a hole ahead of the crack tip.

Figure-11(a) shows crack extension behavior under mode I loading occurred in opening type fracture. Here, fracture surface near the surfaces of the specimen occurred with shear lip; however the fracture surface was flat in the mid thickness. In this case, the appearance of the whole fracture surface was not flat due to the grain orientation does alter the crack growth process on a local level. Fracture behavior under mixed mode with loading angle 45^o is shown in Figure-11(b). In this case, crack initiation occurred in opening fracture. Furthermore, crack extension propagates due to the critical value of shear stress, then shear fracture occurs due to critical shear stress at ligament. In the pure mode II loading with loading angle 0^o (Figure-11 (c)) crack initiation and propagation occurred only due to shear fracture and the fracture surface was flat.

It was found that, effect of a small hole on the crack propagation behavior for all cases, indicated that the load was drop after crack propagation coalesces to the hole.

From these results, it could be inferred that the existence of a small holes ahead of the crack tip could decrease the ligament between crak tip and the hole due to

crack extension then shear type fracture instability occurred.

CONCLUSIONS

Fracture behavior under mode I up to a certain value of mixed mode loading indicated that the crack initiation and propagation direction perpendicular to the loading direction. On the contrary, crack growth behaviors under mode II loading show that the shear fracture occurs near the crack tip. The fracture resistance is influenced by the rolling direction of the material and its value is smaller in the rolling direction than other direction.

In the mixed mode fracture tests with the mode II component is dominant, the crack initiation occurs in shear type fracture. Therefore, the fracture criterion did not follow the maximum hoop stress criterion. Shear fracture instability occurs at the ligament when the shear stress is over the shear strength of the material. Since the appearance of a small hole ahead of the crack tip affected the crack growth behavior, and then crack propagation coalesces to the hole direction by shear type fracture.

REFERENCES

[1] F. Erdogan and G.C. Sih. 1963. On the Crack Extension in Plates under Plane Loading and Transverse Shear. Journal of Basic Engineering. 85: 519-525.

[2] N. Halbäck and F. Nilsson. 1994. Mixed mode I/II Fracture Behavior of an Aluminum Alloy. Journal Mechanics Physics Solids. 42(9): 1345-1374.

[3] S. Aoki, K. Kishimoto, T. Yoshida, M. Sakata and H. A. Richard. 1990. Elastic-Plastic Fracture Behavior of an Aluminum Alloy under Mixed mode loading. Journal Mechanics Physics Solids. 38(2):195-213.

[4] Husaini, and K. Kishimoto. 2000. Mixed mode Fracture Behavior of PC/ABS Blends. Proceedings of the 2nd International Conference on Experimental Mechanics 2000. Singapore, pp. 111-116.

[5] Husaini, K. Kishimoto, M. Notomi and T. Shibuya. 2001. Fracture Behavior of PC/ABS Resin under Mixed Mode Loading. Journal Fatigue Fracture Engineering and Materials Structure. 24(12): 895-903.

[6] Husaini, M. Notomi, K. Kishimoto and T. Shibuya. 1997. Crack Initiation Behavior of ABS Resin Under Mode I and Mixed Mode Loading. Materials Science Research International. 3(3): 158-165.

[7] JSME. 1981. Standard Method of Test for Elastic-Plastic Fracture Toughness J_{IC}-S001-1981.

[8] H.A. Richard and K. Benitz. 1983. A Loading Device for the Creation of Mixed mode in Fracture Mechanics. International Journal Fracture. 22: R55-58.

[9] T.L. Anderson. 1991. Fracture Mechanics Fundamentals and Application. CRC Press. Inc., Boca Raton Ann Arbor Boston.

[10] 1994. MARC Analysis Research Corporation, MARC User's Manual. California 94306 USA.

[11] Y. Murakami. 1987. Stress Intensity Factor Handbook. Pergamon Press. l.2: 929-930.

[12] Husaini, M. Notomi, K. Kishimoto and T. Shibuya. 1997. Crack Initiation Behavior of ABS Resin Under Mode I and Mixed Mode Loading. Materials Science Research International. 3(3): 158-165.